

Short communication

Influence of cooling treatment on corrosion behaviour of steel EH40 in extremely cold seawater

Hengding Li, Yaohua Dong*, Yuanyuan Shen*, Xueting Chang, Dongsheng Wang, Xiaofeng Li, Yansheng Yin

Institute of Marine Materials Science and Engineering, College of Ocean Science and Engineering, Shanghai Maritime University, Shanghai, 201306, China

*E-mail: yhdong@shmtu.edu.cn, yyshen@shmtu.edu.cn

Received: 26 May 2017 / *Accepted:* 25 September 2017 / *Published:* 12 November 2017

The corrosion resistance of low-temperature steel EH40 with and without cooling treatment was investigated after salt spray testing under artificial conditions. The surface morphologies, chemical compositions, and corrosion rates of low-temperature steels EH40 were respectively analyzed by scanning electron microscopy (SEM), energy dispersive spectrometry (EDS), and mass loss method. Electrochemical impedance spectroscopy (EIS) measurements were employed to examine the effect of the cooling treatment on the corrosion mechanism of EH40. The results showed that pitting corrosion occurred for the steels subjected to cooling treatment at -80°C , which further accelerated their corrosion behaviors. By contrast, a uniform corrosion pattern was observed on the steel samples unsubjected to the cooling treatment. In the latter case, the formation of passive films on the steels surfaces lowered the rates for further corrosion.

Keywords: EH40 steel; Cooling treatment; Low-temperature seawater corrosion; Pitting

1. INTRODUCTION

The discovery of large amounts of gas hydrates in the cold polar regions of the earth has recently attracted worldwide concerns [1-2]. The paucity of knowledge about the polar region led researchers to use a variety of techniques to expand the available information to cover the entire continent. Particular polar expedition vessels [3-5] are often used to navigate under the lower temperature atmosphere. Therefore, low-temperature steels which resist to very cold polar conditions are required to construct polar expedition vessels.

The impact fracture toughness of materials at low temperature greatly changes, where materials suffer from brittle rupture [6-7]. A number of studies showed that low temperature and welding

remarkably influence steel track fracture [8-9]. For example, fracture behavior of porous iron at temperatures ranging from room to -60°C was examined by Straffelini et al [10], and the results revealed that the impact fracture toughness increase as the testing temperature decrease. Menzemer et al [11] found that the extrinsic influence of temperature on impact toughness–fracture resistance could be explained by the mutual interactive influences of intrinsic microstructural features, local stress states, and macroscopic fractures. To date, although some steel plates with excellent brittle crack arrestability for shipbuilding have been accomplished [12-14], low-temperature steels performing at extremely cold conditions like polar environments still require development.

In particular, EH40 steels were shown to have great potential in building polar expedition ships due to their high strength performance, relevant low-temperature impact toughness, prominent ship plate steel extension, and outstanding weldability. Two main properties of EH40 steels are currently investigated more than the others, and this relies on low-temperature toughness and high-efficiency welding process. Ma et al [15] demonstrated that EH40 thick steel plates have excellent toughness at low temperatures (-10°C) using tests based on CTOD (crack tip opening displacement). Fatigue crack growth rates in EH40 steels were evaluated by Xia et al [16], and a new crack propagation rate formula was established. Other studies found that the impact toughness property of EH40-TM steel plates welded with high heat input was linked to the microstructure morphology, distribution of grain boundary ferrite, and the acicular ferrite [17-18]. High strength steel plates with heavy gauges of EH36, EH40 and EH47 grades weld with high heat input were explored, and the data suggested the steel plates have excellent mechanical properties in terms of base plates and welded joints [19].

To date, the structural properties and performance of steels were extensively investigated at high temperatures [20-23] but a little research on steels was performed at low temperatures, especially in extremely cold environments. A survey of the literature revealed that only handfuls of studies are accessible on corrosion behaviors of material under freezing temperatures. The structural and mechanical properties of EH40 steels could resist to lower temperatures but once cracks occur, the properties could sharply deteriorate, especially the corrosion resistance in chloride environments like seawater. Therefore, it is necessary to determine the corrosion behavior of EH40 steels under extreme cold environment.

In this work, the corrosion resistances of EH40 steels were tested with and without cooling treatment. EH40 was firstly cooled to -80°C and then immersed in artificial seawater under low temperature. The corrosion mechanisms of EH 40 were systematically investigated by combined techniques based on scanning electron microscopy (SEM), energy dispersive X-ray spectroscopy (EDS), mass loss, and electrochemical impedance spectroscopy (EIS).

2. EXPERIMENTAL

2.1 Test specimen and test preparation

EH40 steels with planar dimensions of $300\times 500\text{mm}$ and thicknesses of 30mm were supplied by Baosteel Co., Ltd. The compositions of the steels are listed in Table 1.

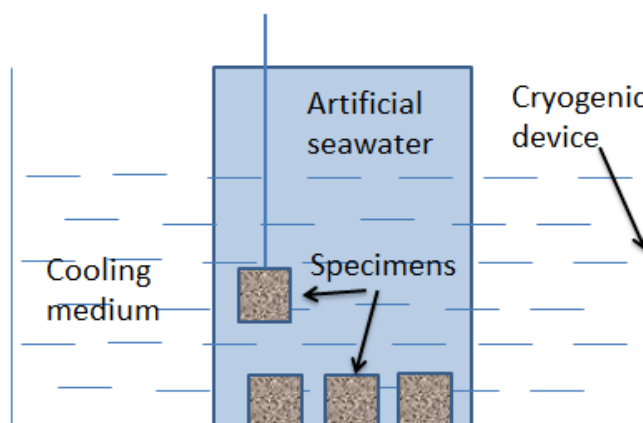
Table 1. Chemical compositions of the tested steels (wt%).

Element	C	Si	Mn	P	S	Cr	Ni	Mo	Cu	Al	Nb	V	Ti	Fe
Content	0.16	0.15	0.90	<	<	0.20	0.40	0.08	0.35	0.015	0.02	0.10	0.02	Balance
				0.010	0.0015									

Rectangular coupons (10mm×10mm×2mm) were cut from the as-supplied steel plates and used for mass loss assay and corrosion analysis. Prior to the experiments, the surfaces of the specimens were ground with silicon carbide (SiC) papers progressively up to 600 grit, rinsed with deionized water and degreased with acetone before drying under a cool air. All the samples were then placed in a desiccator for 24h. Subsequently, the coupons weights were measured by a precise electronic balance (FA 114).

Prior to electrochemical measurements, the specimens were embedded in epoxy resin leaving an exposed testing area of 1 cm². Each coupon surface was wet abraded to an 800-grit finish, degreased with acetone, rinsed with distilled water, and finally dried under a cool air. For comparative purposes, half of the resulting specimens were cooled to -80 for three days, and others were left placed in a desiccator at 25°C.

All the corrosion experiments were carried out with a cryogenic system (DL-2005). The samples with and without cooling treatment were placed in beakers of artificial seawater at temperatures of 0°C±0.2°C. During the tests, sodium chloride (NaCl) solutions with concentrations of 35 g/l ± 5 g/l were used as the artificial seawater. The total test time lasted three days. Three mass loss specimens were tested for each treatment process to calculate the corrosion rates.

**Figure 1.** Schematic diagram of low-temperature artificial seawater immersion tests

2.2 Surface morphology and component analysis

The morphologies of the corrosion products of EH40 steels after the immersion testing for three days were observed by a scanning electron microscope (SEM, JSM-7500F model, 10kV). An energy dispersive spectrometer (EDS) was employed to analysis the compositions of the corrosion products.

2.3 Corrosion rate

After the immersion corrosion experiments, all the specimens were taken out and immediately cleaned with distilled water. To remove the corrosion products, the specimens were put in a bath containing 10% hydrochloric acid (HCl) inhibited with 10 g/L hexamethylenetetramine (urotropine) at room temperature and then rinsed and dried. Next, the samples were weighed again to obtain the final weights and allow calculating the weight loss values. The corrosion rate was estimated according to Eq. (1).

$$V_{\text{corr}} = \Delta m / (S * t) \quad (1)$$

where V_{corr} is the corrosion rate in $\text{mg} \cdot \text{dm}^{-2} \cdot \text{d}^{-1}$, Δm is the weight loss in g, S is the surface area of the specimen in dm^2 , and t is the corrosion time in days (d). The final corrosion rate was taken as the average of two measurements after three days of corrosion testing, and the data were presented with error bars.

2.4 Electrochemical measurements

The electrochemical impedance spectroscopy (EIS) was performed using an electrochemical workstation (Metrohm AG Autolab) and the data were fitted with Auto lab equipped with software Nova 1.10. A conventional three-electrode glass corrosion cell was used. A saturated calomel electrode (SCE), a piece of platinum with an area of 2.25 cm^2 and low-temperature steel sample were used as the reference electrode, counter electrode, and working electrode, respectively. The test medium contained 3.5 wt.% sodium chloride solution to mimic sea water during the corrosion process. Before EIS measurements, the specimens were immersed in the salted media for 30min at room temperature to make sure the testing process was stable. The EIS measurements were conducted at frequencies ranging from 10kHz to 10mHz at open circuit potential (OCP) with voltage perturbation of $\pm 5 \text{ mV}$.

3. RESULTS AND DISCUSSION

3.1 Surface morphological and corrosion product analysis

Fig. 2 shows the SEM images of the EH40 specimen surfaces with and without cooling treatment after the immersion corrosion process for three days. The surfaces of specimens unsubjected to the cooling treatment appeared with uniform films, while those subjected to the cooling treatment at -80°C looked loosen and asymmetry. The corresponding SEM pictures presented in Fig. 3 after the corrosion products were removed from the corrosion coupons. Fig. 3 clearly depicted that the specimens unsubjected to the cooling process underwent a uniform corrosion after the salt spray for three days while the samples subjected to the cooling process experienced pitting corrosion.

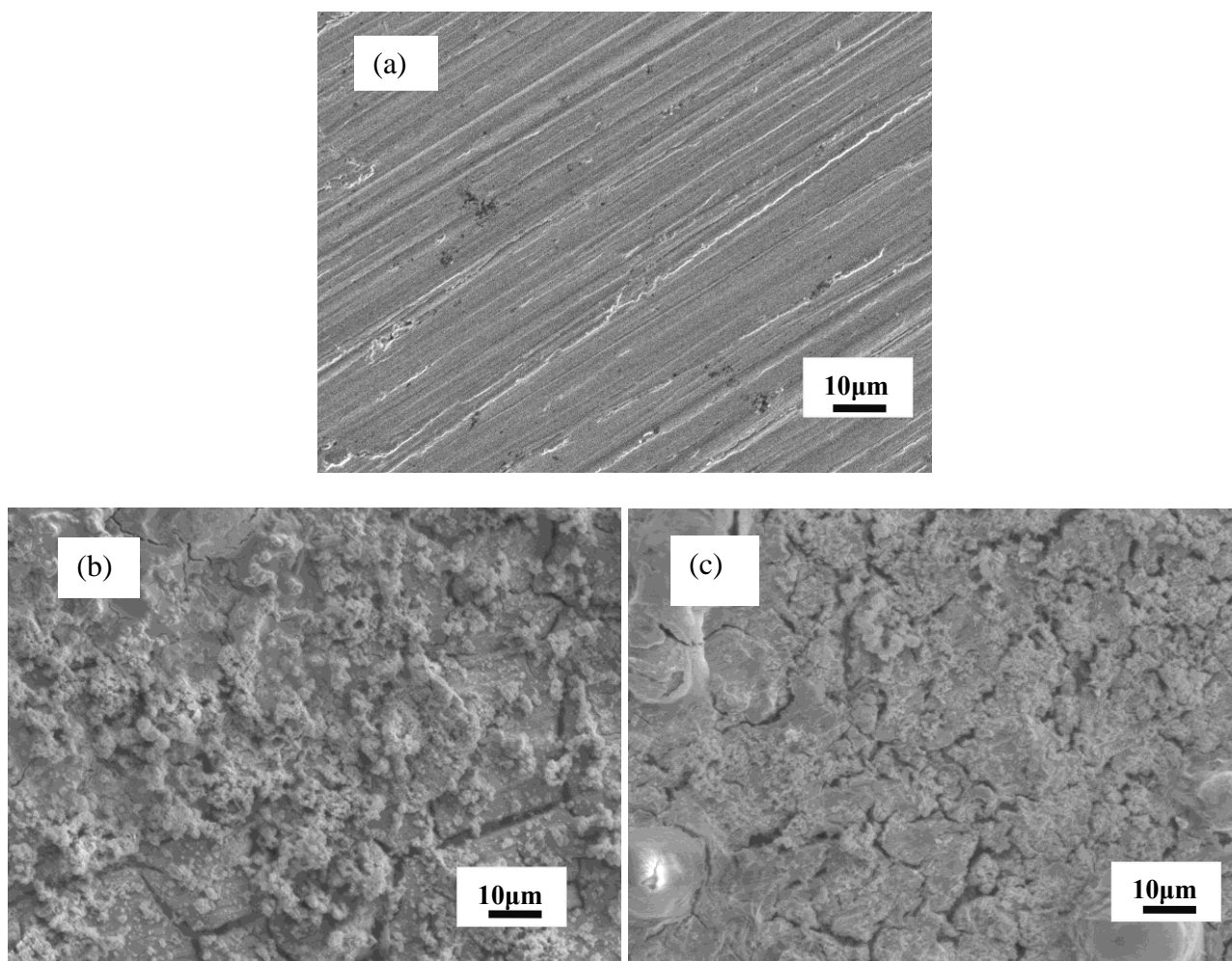


Figure 2. SEM images of surfaces of the EH40 specimens before and after the immersion corrosion tests: (a) specimen before the tests, (b) corrosion products of the cool-treated specimens after the immersion, (c) and corrosion products of the specimens unsubjected to the cooling treatment after the immersion.

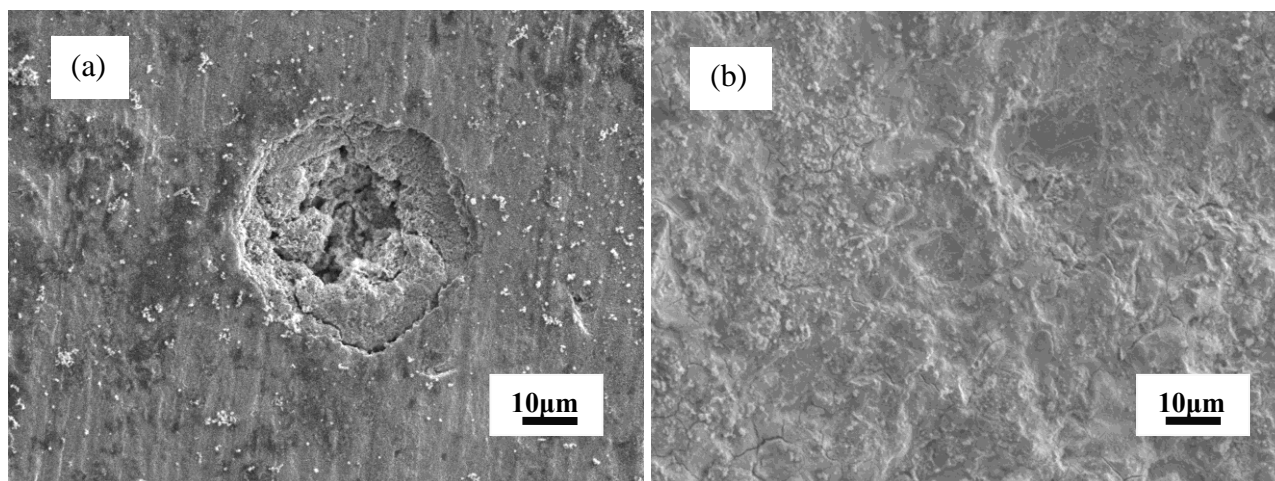
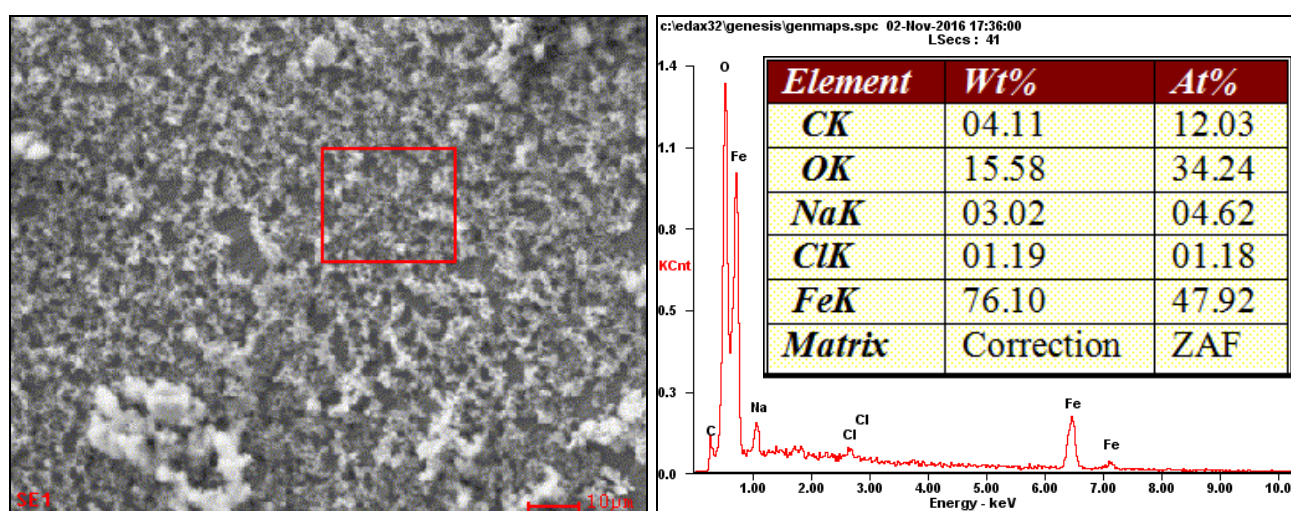


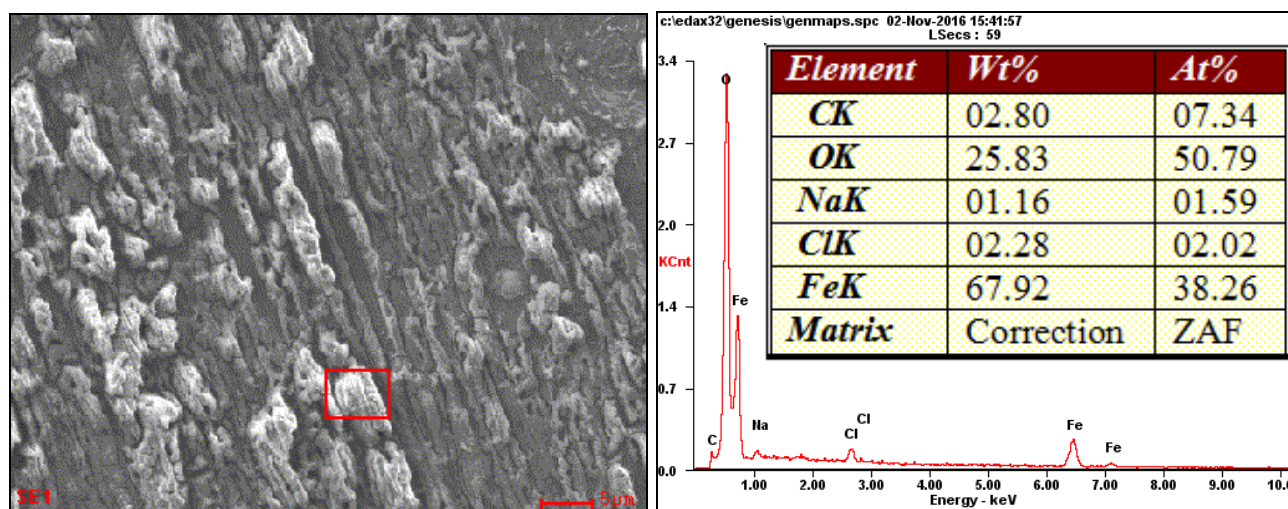
Figure 3. SEM images of the specimens after removal of the corrosion products: (a) cooling treatment at -80°C and (b) unsubjected to cooling treatment.

Fig.4 depicts the chemical composition of the corrosion products performed through EDS. The primary elements present in the corrosion products were O and Fe with a trace of C, Cl, and Na. Therefore, it can be proposed that the corrosion products were mainly composed of iron oxides. The data also suggested that O and Cl contents in the specimens unsubjected to the cooling treatment were higher than those of the treated samples which demonstrated that the corrosion products were much more.

Previous studies [24-25] demonstrated that uniform and dense corrosion products formed on steel surfaces could be effective as anti-corrosion protective films as the corrosive substances are not in direct contact with the steel surface. Thus, passive corrosion films might protect steel from further corrosion and decrease the corrosion rates.



a. -80°C



b. 25°C

Figure 4. SEM images and the corresponding EDS spectra of specimens with and without cooling treatment after immersion 3 days.

However, corrosion pits were found on the steel surface of the samples subjected to the cooling treatment at -80°C after removal of the corrosion products (Fig. 3). Cl^{-} is considered as the most aggressive ion species present in artificial seawater, which could destroy the formed oxide layers [26] to easily penetrate the loosen products film. Cracks occurred easily in the cooled specimens at -80°C , hence Cl^{-} diffused to reach the internal structures of the specimens, which led to serious local corrosion. Once the enriched Cl^{-} concentration exceeded a threshold in a local region of the steel specimen, a new pitting corrosion could possibly be initiated. By contrast, the formation of an anti-corrosion protective film on the samples unsubjected to the cooling process restrained further corrosion.

3.2 Corrosion rate analysis

The average corrosion rates of different specimens were calculated based the mass loss and the data are shown in Fig. 5. The corrosion rate of samples subjected to the cooling treatment at -80°C was estimated to $22.62\text{mg}\cdot\text{dm}^{-2}\cdot\text{d}^{-1}$, which was higher than the value ($19.88\text{mg}\cdot\text{dm}^{-2}\cdot\text{d}^{-1}$) of untreated samples. SEM and EDS confirmed that the corrosion products formed on the surfaces of specimens subjected to the cooling process appeared uniform and compact, suggesting a uniform corrosion. By comparison, the surface of specimens subjected to cooling process showed pitting corrosion underneath the loosen corrosion, which could not be identified without removing the surface products. As a result, the steel substrate was subjected to severe corrosion at the later stages of test.

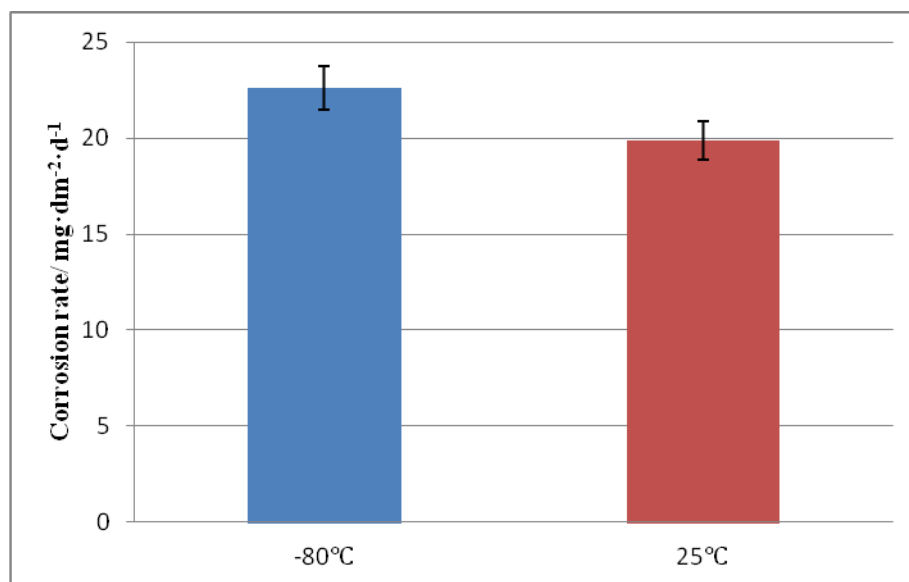


Figure 5. Corrosion rates of different treated EH40 steel after 3 days of immersion corrosion testing.

3.3 Electrochemical studies

Electrochemical impedance spectroscopy (EIS) is a powerful and non-destructive technique used for characterization of electrochemical reactions at the metal/electrolyte interface and study

corrosion products formation. The impedance spectra are normally displayed either in the form of a Nyquist (complex plane) plot or a Bode plot [27]. Herein, the impedance spectra of cooling treated and untreated steel samples were recorded at the open circuit potential to monitor the corrosion behavior.

Fig. 6 illustrates the impedance spectra of different treatment steel samples after 3 days of immersion corrosion testing. Compared to original steel unsubjected to immersion at low temperature, Fig. 6a clearly showed that diameters of the impedance loops after the immersion corrosion for three days significantly decreased. Also, the diameters of impedance loops of the cooling treated sample appeared smaller than those of untreated specimens implying the acceleration in the corrosion rates of the steel specimens. These differences in impedance loop diameters could be attributed to the corrosion films formed on the surface of the steel samples without cooling treatment. The respective magnitude Bode plot (Fig. 6b) illustrated that the total impedance magnitude at the lowest frequency of uncooling-treated steels (the logarithmic value was 2.3) was higher than that (the logarithmic value was 2.1) of cooling-treated ones. As shown in the phase angle Bode plots (Fig. 6c), a weak phase angle maximum appeared at the lowest frequency range of cooling-treated steel specimen, implying active pit growth [28]. Previous studies revealed that steel treated at -80°C induced pitting corrosion underneath the corrosion products, which were consistent with the electrochemical results.

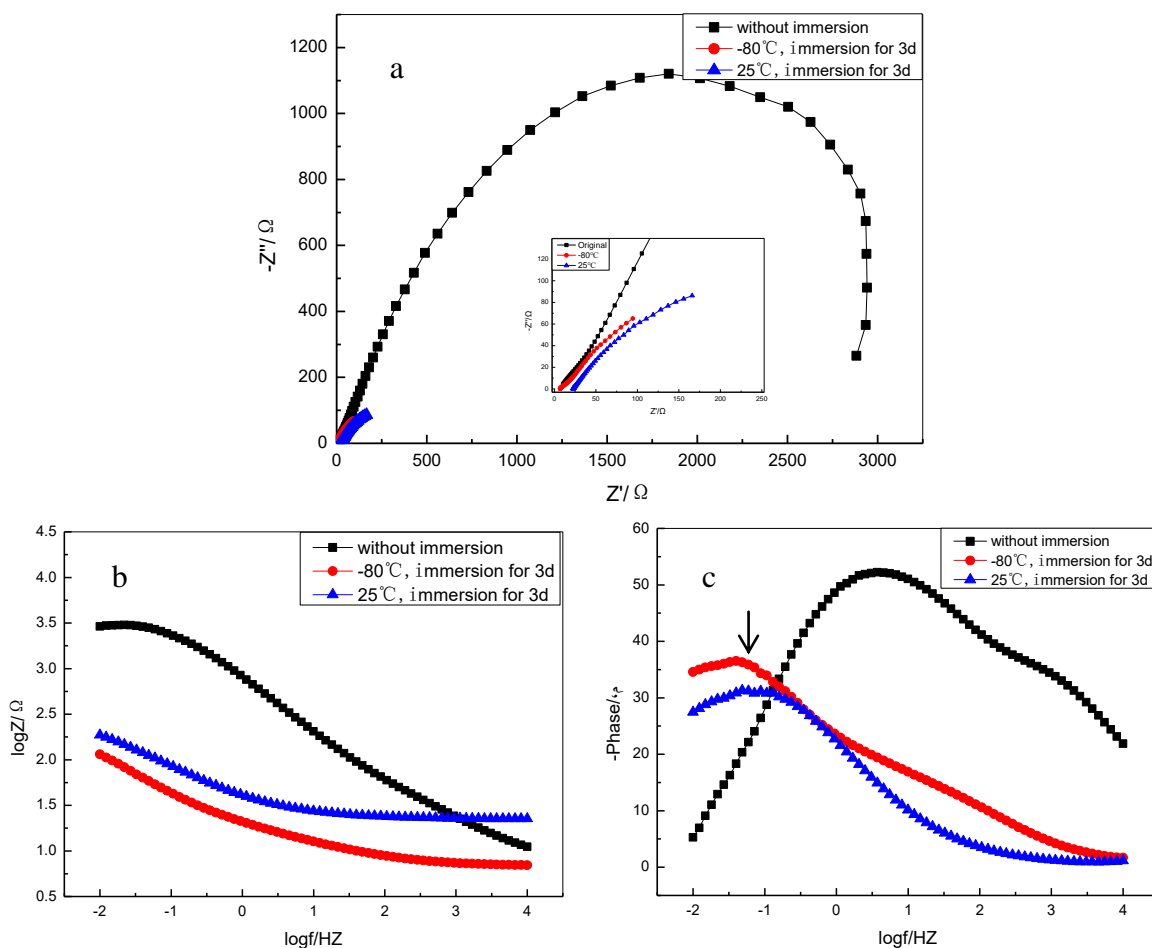


Figure 6. Impedance spectra of different treated low-temperature steels after 3 days of immersion corrosion testing at the open circuit potential.

Usually, impedance spectra are analyzed using an equivalent circuit, taking into account the contribution of each phenomenon, such as EDL, film formation, coating and others. The corrosion characteristics of steel under low-temperature artificial seawater atmosphere were further analyzed using the impedance data based on two equivalent circuits (Fig. 7) [29]. In the equivalent circuits, R_s is the solution resistance, CPE_f and R_f are respectively the capacitance and resistance of the passive corrosion products formed during corrosion testing, R_{ct} is the charge transfer resistance, CPE_{dl} represents the double-layer capacitance at the surface of the electrolyte/steel substrate, and CPE_{dl} and CPE_f are the constant phase angle elements used as substitute of capacitor to compensate non-homogeneity in the system. The first equivalent circuit was used to fit the EIS data with only one capacitive loop (Fig. 7a) but the second circuit was used for EIS data with two capacitive loops (Fig. 7b).

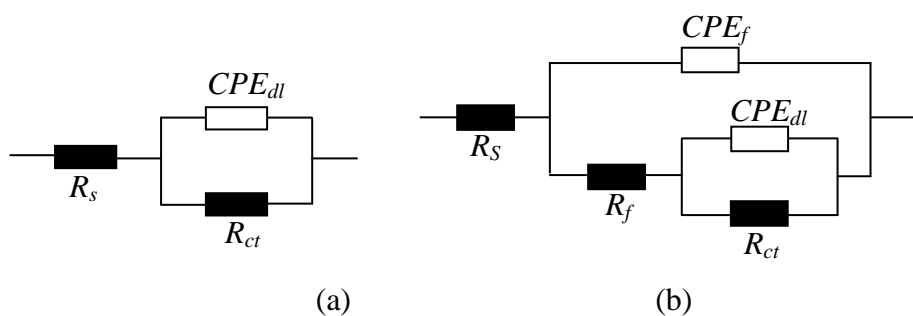


Figure 7. The two equivalent circuits used for fitting the impedance data of the steel specimens in salt spray atmosphere: (a) fitting data with only one capacitive loop and (b) fitting data with two capacitive loops.

The fitted parameters of the electrical components are listed in Table 2. As can be seen, the charge transfer resistances (R_{ct}) of the specimens subjected to the cooling process were smaller than those of untreated steel samples. It is widely recognized that the corrosion rate is inversely proportional to changes in transfer resistance based on the Stern-Geary equation [30-32]. The results implied higher corrosion rates of the cooling-treated steel samples which underwent the cold immersion process. Moreover, the charge transfer resistances (R_{ct}) of specimens after the immersion corrosion were much less than those of original steel which not immersed. This demonstrated that despite the formation of uniform film on the surface of samples unsubjected to the cooling treatment after immersion corrosion, the corrosion rates of these steels were still higher than those of original steels without low temperature immersion. Another noticeable circuit element in Table 2 deals with the resistance of oxide films (R_f). Compared to the specimens cooling treated, the R_f of the specimens unsubjected to cooling treatment was higher, which suggested that the oxide films gradually grew after corrosion to form thick and compact layers on the surface of not cooling treated steel (Fig. 8a).

The cool-treated EH40 steels at -80°C tended to generate crack originated early in the process, and then extended on the surface[13]. By comparison, the steel unsubjected to the cooling treatment showed no cracks. The chloride ions can easily penetrate the cracks to infiltrate the inner layers of steel and cause pitting corrosion (Fig. 8b). As the chloride ions had no access to the inner layers of not

cooling treated steels, the corrosion products were homogeneously formed on the surface of the EH40 steel (Fig. 8a).

Table 2. Fitting parameters of impedance spectra of the studied steels.

Sample	$R_s(\Omega)$	CPE_{dl}	n_1	$R_{ct}(\Omega)$	CPE_f	n_2	$R_f(\Omega)$
Original	9.53	323	0.625	3330	---	---	---
80°C(3d)	22.4	16.8	0.522	389	---	---	20.1
25°C(3d)	6.74	22.3	0.626	432	15.4	0.489	22.4

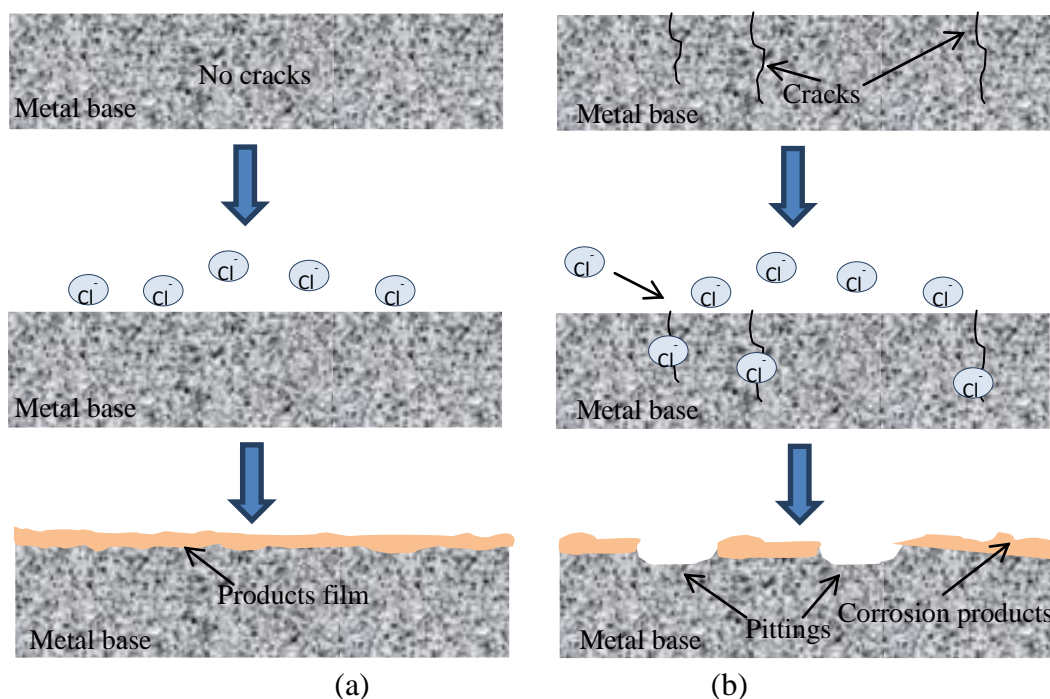


Figure 8. The corrosion mechanism of EH40 in the low-temperature artificial seawater environment: (a) without cooling treatment and (b) with cooling treatment at -80°C .

The corrosion behavior was further confirmed by analyzing the obtained open circuit potentials (OCPs), as shown in Fig. 9. During corrosion, the OCP negatively shifted but the shifts recorded with the untreated samples were less than those of specimens subjected to cooling process. This confirmed the formation of a passive film on the surface of the not cooling treated specimens, slowing down the corrosion rates of further oxidation. By contrast, pitting corrosion formed on the specimens subjected to cooling treatment, thus leading to further severe corrosion. These phenomena can cause shifts in OCP towards the negative direction and decrease the anti-corrosion process. These results were also consistent with the previous corrosion morphology.

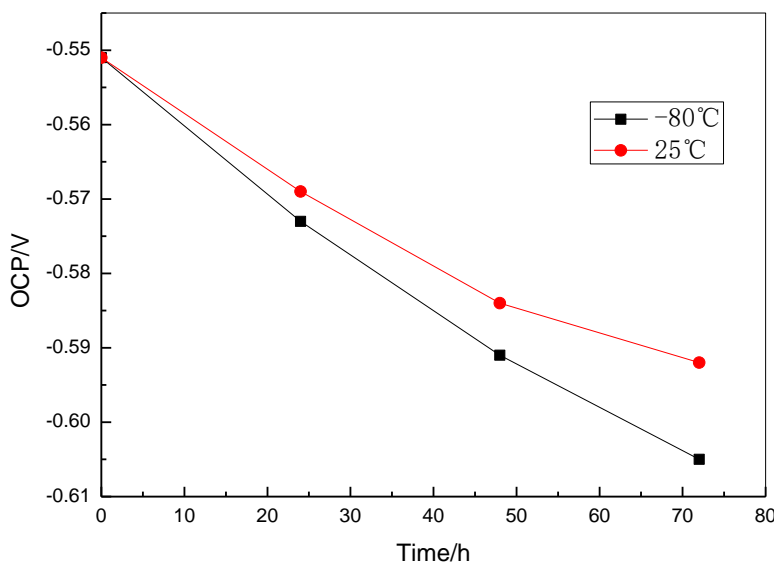


Figure 9. The open circuit potentials (OCPs) of cool-treated and untreated steels after immersion corrosion for three days.

4. CONCLUSIONS

The corrosion behaviors of EH40 steels with and without cooling treatment in low-temperature artificial seawater atmosphere for three days were investigated by means of SEM/EDS, mass loss, and EIS techniques. The specimens subjected to cooling treatment at $-80\text{ }^{\circ}\text{C}$ showed signs of pitting corrosion, which later led to further serious corrosion. By comparison, the steel samples unsubjected to the cooling treatment experienced uniform corrosion with the formation of anti-corrosion passive films, which prevented further corrosion under the testing atmosphere. On the other hand, the anti-corrosion properties of steels decreased under artificial seawater environment compared to original steel samples unsubjected to the low-temperature salty conditions. Overall, these findings suggest that at low temperatures combined with salty conditions, more attention should be paid as corrosion processes could be accelerated, and thus better preventive measures should be considered.

ACKNOWLEDGEMENTS

The authors acknowledge the financial support of the National Natural Science Foundation (No. 51609133 and No. 5162195) and National Key Research and Development Program (No. 2016YFB0300700).

References

1. K. A. Kvenvolden, *The Future of Energy Gases*, 1570 (1993) 279.
2. T. S. Collett, *AAPG Bulletin*, 86 (2002) 1971.
3. T. S. Collett, A. H. Johnson, C. C. Knapp, R. Boswell, *AAPG Memoir* 89 (2009) 146.
4. N. V. Cherskiy, V. P. Tsarev, S. P. Nikitin, *Petroleum Geology*, 21 (1985) 65.
5. T. S. Collett, M. W. Lee, W. F. Agena, *Marine and Petroleum Geology*, 28 (2011) 279.

6. Q. X. Dai, A. D. Wang, X. N. Cheng, *Advances in Materials Science and Engineering*, 311 (2001) 205.
7. J. Bystrzycki, R. A. Varin, *Advances in Materials Science and Engineering*, 270 (2001) 151.
8. B. R. Feng, Y. Q. Wang, Y. J. Shi, *Low Temp. Arch. Tech.*, 4 (2005) 97.
9. X. N. Cheng, Q. X. Dai, A. D. Wang, *Advances in Materials Science and Engineering*, 311 (2001) 211.
10. G. Straffelini, V. Fontanari, A. Molinari, *Advances in Materials Science and Engineering*, 272 (1999) 389.
11. C. C. Menzemer, T. S. Srivatsan, R. Ortiz, *Materials & Design*, 22 (2001) 659.
12. Y. Murakami, Y. Takeuchi, K. Hase, *International Journal of Off Shore and Polar Engineering*, 24 (2013) 286.
13. K. Nakashima, K. Hase, S. Endo, T. Eto, H. Fukai, *International Journal of Off Shore and Polar Engineering*, 53 (2014) 26.
14. H. J. Jae, Y. H. Ja, W. L. Hae, *Korean Journal of Metals and Materials.*, 51 (2013) 33.
15. M. Tao, Z. X. Cao, X. J. Chen, *Ship & Ocean Engineering*, 39 (2010) 230.
16. Z. J. Xia, Z. M. Miao, J. Zhu, *Steel Construction*, 30 (2015) 32.
17. T. G. Park, J. M. Kim, H. Y. Yoon, *Korean Journal of Metals and Materials*, 48 (2010) 1021.
18. P. Y. Zhang, C. R. Gao, F. X. Zhu, *ACTA Metallurgica Sinica*, 48 (2012) 264.
19. C. S. Lee, S. Kim, I. Suh, K. K. Um, O. Kwon, *Journal of Iron and Steel Research, International*, 18 (2011) 796.
20. S. Roychowdhury, H. P. Seifert, P. Spätig, *Journal of Nuclear Materials*, 478 (2016) 364.
21. T. Emmerich, C. Schroer, *Corrosion Science*, 120 (2017) 171.
22. K. Sipilä, M. Bojinovb, W. Mayinger, *Electrochimica Acta*, 173 (2015) 757.
23. H. Subramanian, V. Subramanian, P. Chandramohan. M. P. Siiniwasan, S. Rangaraian, S. V. Narasimhan, S. Velmurugan, *Corrosion Science*, 70(2013) 127.
24. Y. Z. Wu, D. J. Kong, D. Long, G. Z. Fu, *Transactions of the China Welding Institution*, 33(2012)101.
25. S.J. KIM, S. K. JANG, *Transactions of Nonferrous Metals Society of China*, 19(2009)50.
26. C. D. Waard, U. Lotz, D. Milliams, *Corrosion*, 47 (1991) 976.
27. S. J. Yuan, S. O. Pehkonen, *Corrosion Science*, 49 (2007) 1276.
28. J.R. Scully, D.C. Silverman, M.W. Kendig, *Electrochemical Impedance: Analysis and Interpretation*, ASTM, (1993), Philadelphia, 297.
29. X. H. Zhang, S. O. Pehkonen, N. Kocherginsky, G. A. Ellis, *Corrosion Science*. 44 (2002) 2507.
30. B. A. Boukamp, *Equivalent Circuit Users Manual*, University of Twente, (1993) Netherland.
31. Y. S. Tan, M. P. Srinivasan, S.O. Pehkonen, Y. M. Chooi, *Corrosion Science*. 48 (2006) 840.
32. J. R. Macdonald, *Impedance Spectroscopy-Emphasizing Solid Materials and Systems*, Wiley, (1989) New York, American.